

Grid Connected Wind Energy Conversion System for Peak Load Sharing Using Fuzzy Logic Controller

Muhammad Mansoor Ashraf*, Abu Bakar Waqas*‡, Tahir Nadeem Malik*

* Department of Electrical Engineering, Faculty of Electronics and Electrical Engineering, University of Engineering and Technology Taxila (47050), Pakistan

(mansoor.ashraf@uettaxila.edu.pk, abubakar.waqas@uettaxila.edu.pk, tahirnadeem03@gmail.com)

‡ Corresponding Author; Abu Bakar Waqas, Department of Electrical Engineering, University of Engineering and Technology Taxila (47050), Pakistan. Tel: +92 51 90 47 540, Fax: +92 51 90 47 420, abubakar.waqas@uettaxila.edu.pk

Received: 01.04.2017 Accepted: 20.08.2017

Abstract- The rapidly growing use of renewable energy sources in context of smart grid environment entails the power system operational planning, optimal allocation, sizing and robust control of Distributed Generators (DGs). In this regard wind energy systems are getting an immense attention of researchers in the recent decade. In this research paper, an efficient Pitch Frequency Control (PFC) mechanism based fuzzy logic control technique has been proposed for peak load sharing of utility supply. The controller is activated and employed to integrate the wind energy system (WES) with utility supply to take up additional peak load along with the regulation of shaft speed of turbine and thus electrical frequency of the generator against load variations and uncertain wind blows. The proposed technique has been modelled and simulated in Simulink environment of MATLAB to analyse and investigate its performance. The results show the improved performance for PFC of wind energy system by minimizing the percent overshoot and settling time of the output. Thus the proposed technique reflects its significance by its application for wind energy systems consisting of low speed electrical generators.

Keywords Wind energy system, fuzzy controller, blade pitch control, peak load sharing, utility supply.

1. Introduction

The tremendously increasing cost of fossil based fuels and their hazardous impacts on environment are the major intentions for which conventional energy sources are being promptly substituted by renewable energy resources. Increased efficiency of PV cell due to improvement in its design parameters has led the world to employ PV systems as one of reliable energy source. PV systems are often used standalone or in grid connected mode with variation of loads [1]. In [2] the different challenges such as geography, weather, grid configuration, local workforce, and limited supply chain are described for the grid connected operation of PV system. It also highlights the opportunities which awaits for each challenge and potential waste management strategies.

The wind energy is another well addressed aspect and has become prominent with its applications among the renewable energy resources [3, 4]. A new concept has been elaborated in [5] for innovative hidden wind farms in

suburban households having roof-mounted wind arrester to emphasize the importance of wind energy system. An application of small scale wind turbine can generate 2.90 GWh approximately per year per wind arrester. M. Caruso et. all [6] presents the experimental characterization of wind generator prototype used for micro wind farms with advantages of low noise, versatility, generation of 1kW power for wind speed of 1 m/s. Hybrid Wind-PV power plant can also be used with many benefits such as maximization of renewable fraction, reducing the disadvantages of wind energy integration to the grid, and as a cost effective solution [7]. Generally wind energy systems are classified into three types: domestic wind turbine (less than 10 kW), standalone wind turbine (10 – 500 kW) and conventional wind turbine (500 kW – 5 MW) [8]. The conventional and standalone wind turbines can be synchronized to national grid to deliver electrical energy [9]. There are techniques present in literature for grid connected wind energy systems.

In most cases, the different types of AC-DC-AC converters are being deployed actively for national utility

connected wind energy systems [10]. The existing grid connected inverter systems for small wind turbines result in limited speed range due to limited dc voltage window and high cost as additional control circuitry is required [11-14]. The single stage matrix converter (AC-AC) has been presented for grid connected wind turbine which reduces the power conversion stages and hence reduce the cost and improve the efficiency of system over conventional wind energy conversion systems [15]. The different algorithms and codes of phase locked loop has been proposed for synchronization of wind energy system to utility supply under distorted conditions. It is observed that only Enhanced phase locked loop gives better result as compared to synchronous reference frame and quadrature phase locked loop under harmonic disturbances and grid faults [16]. The wind energy systems are anticipated to be connected to utility by means of high voltage and direct current (HVDC) transmission lines with the help of converter (star-to-delta converter) [17]. The wind energy systems comprising of doubly fed induction generators may also be connected to grid directly as well as through power electronic converters.

The proposed technique work well for wind turbine grid synchronization under low voltage as well as for faults [18]. A novel controller has been developed for induction generator of wind turbine for synchronizing and switching perspectives based on the current flow measurements [19]. The wind turbine coupled with synchronous generator (permanent magnet) along with power electronic converters, has been considered for synchronization. It is observed that closed loop control strategy is slower but adapts the arbitrary changes in the system components whereas open loop is three times faster but unable to adapt system variations [20]. A buck boost converter has been designed for wind turbine consisting of permanent magnet synchronous generator for utility-connected scenario and PI controller is designed to maintain the output voltage of the converter for rotor speed variations [21].

Multi Level Inverter based Static Compensator and active filter topology has been presented in [22, 23] to diminish the effects of power quality issues. STATCOM with a battery energy storage system employs Hysteresis Current Controller which takes care of the reactive power constraint of the load and the induction generator, thus improving the source side power factor and also there will be a noticeable reduction in the Total Harmonic Distortion. An improved Synchronous Reference Frame control has been presented for Dynamic Voltage Restorer (DVR) to upgrade the dynamic response of wind energy system. DVR can effectively lessens voltage dips at the generator terminals and support the wind turbine to stay coupled even under irregular conditions [24].

Most often, the blade pitch control method is employed to regulate the output frequency of electrical generator as well as the shaft speed of wind turbine against load variations and variable wind speed. The proportional integral differential (PID) controller is discussed for pitch control of wind turbine and fuzzy PID controller is designed which greatly reduce the percent overshoot under variable wind speed [25]. The Blade Pitch Control (BPC) system has been

proposed for wind energy systems against peak load sharing together with utility supply. The BPC system basically composed of two independent PI controllers for loading and unloading of wind turbine in specified load intervals [9]. The disadvantage of this controller is that two independent PI controllers are required and the case study only considers one peak in variable load. It is difficult to conclude that how the controller will act or tune itself if another peak occurs in the load, although it greatly reduces the percent overshoot under different load conditions.

In this research paper, fuzzy logic based control technique has been presented for blade pitch control of wind turbine against variable load using PFC. The simulation results show that proposed Fuzzy Logic Control technique exhibits the smoother and improved results. The percent overshoot in the output power curve of the wind energy system has been reduced to 1.0% as compared to presented in [9, 25, 26].

The comprehensive model for simulation has been developed in Simulink environment of MATLAB which includes the modelling of Fuzzy Logic Control technique, wind energy system, utility system, variable load and load management unit. Moreover, the wind energy system follows a set of predefined climatic conditions specified in modelling of wind turbine to be installed at certain site and to exhibit the operational characteristics accordingly [9]. In this research, a conventional wind turbine has been considered which is interconnected to synchronous generator through gear box. The whole system is synchronized to grid supply to take peak load demand during peak load hours by adjusting blade pitch angle using Fuzzy Logic Control system. The simulation results have been analysed in detail and parameter of percent overshoot has been computed and compared.

The rest of the paper is organized as: modelling of wind energy system, utility supply, variable load, load management unit and Fuzzy Logic Control system have been presented in section 2, 3, 4, 5 and 6 respectively; section 7 describes the simulation model; section 8 unveils the simulation results and section 9 concludes the research paper.

2. Modelling of Wind Energy System (WES)

The WES comprises of two essential constituents of wind turbine and electrical generator connected through gear box.

2.1. Wind turbine

All Wind turbine excerpts the energy from blowing wind and converts it to mechanical energy in form of rotating shaft. There are different parameters of wind turbine as: input parameters include blade pitch angle, wind speed and various measurement whereas output parameters are torque, mechanical power and shaft speed etc. The mechanical power developed at the rotating shaft of wind turbine is governed by: [8, 9]

$$P_m = \frac{1}{2} \rho_a A V_w^3 C_p (\lambda, \beta) \quad (1)$$

At sea level and at temperature of 15°C, the International Standard Atmosphere (ISA) defines the density of air as given by: [27]

$$\rho_a = 1.225 \text{ kg/m}^3 \quad (2)$$

Swept area of the wind turbine is the area of the blades that faces the air effectively. If blade length is measured, the swept area can be calculated by: [9]

$$A = \pi R^2 \quad (3)$$

The ratio of speed of tip of blade to speed of wind is defined as Tip Speed Ratio (TSR) and is denoted by λ [9, 27, 28].

$$\lambda = \frac{V_T}{V_w} \quad (4)$$

Tip speed of blade is specified as: [9]

$$V_T = \frac{2\pi R}{60} n \quad (5)$$

TSR is function of wind speed and shaft speed for a certain model of wind turbine at constant value of blade pitch [9].

$$\lambda(n, V_w) = \frac{2\pi R}{60} n \frac{1}{V_w} \quad (6)$$

In order to create reasonable lift and drag forces on the blades, the blades have to be positioned and fitted on the hub at an angle with reference to the direction of wind [29]. The specific angle at which all the blades are attached, is referred as Blade Pitch Angle (β). The different components of wind turbine hub are shown in Figure 1. Generally, the blade chord is oriented along the horizontal axis of Frame of Reference (FR) (shown by Figure 1(b), 1(c)) [8, 29-31]. In this research, the blade pitch values $\beta=24^\circ$ and $\beta=104^\circ$ are revealed in Figure 1(d), 1(e) by considering the horizontal axis of Frame of Reference (FR) and Plane of Rotation (PR) parallel to each other [9].

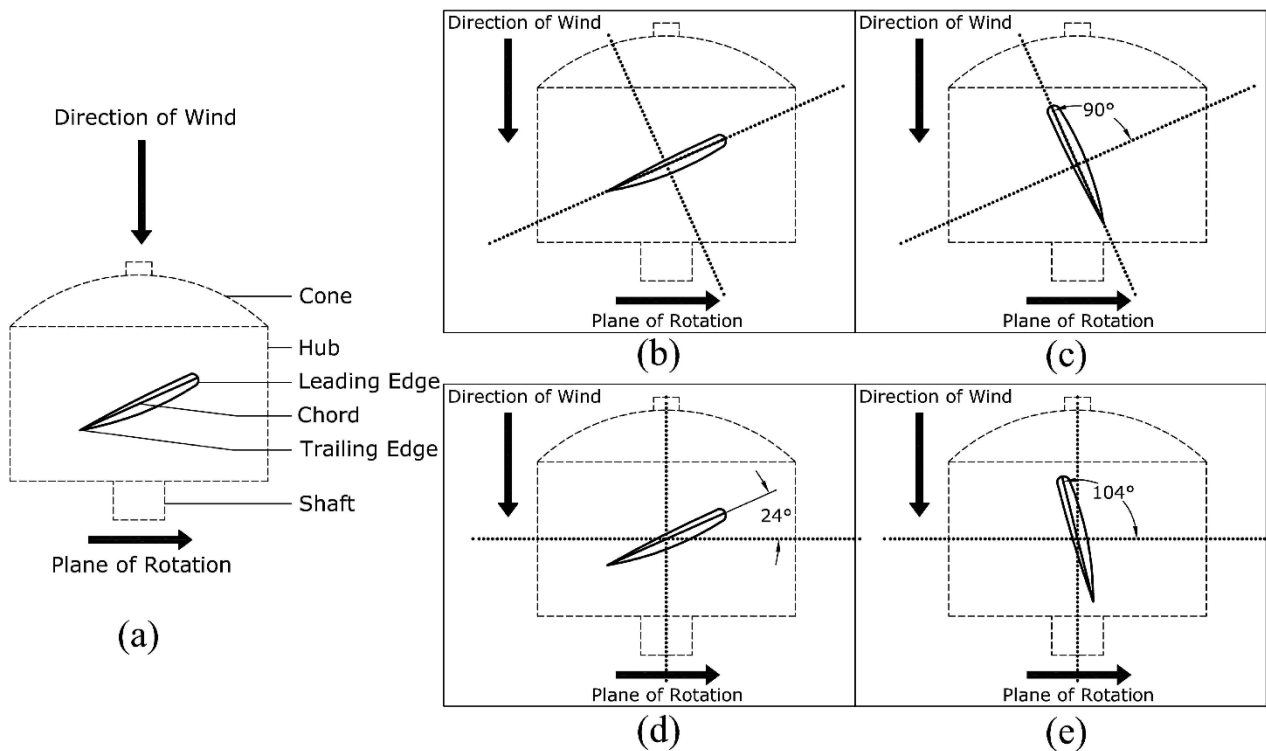


Fig. 1. (a) Components of wind turbine blade, (b) $\beta=0^\circ$ when blade chord and FR are parallel, (c) $\beta=90^\circ$ when blade chord and FR are parallel, (d) $\beta=24^\circ$ when PR and FR are parallel, (e) $\beta=104^\circ$ when PR and FR are parallel

The power coefficient (C_p) is the factor that is defined as extent to which the wind turbine extracts the energy from wind and converts to mechanical energy on the shaft [9]. The number of blades of wind turbine and blade pitch angle determine the value of C_p factor [32]. The maximum value of C_p is specified by Betz limit which is 0.59 and no wind turbine crosses this limit. C_p is a function of blade pitch angle and TSR [8].

$$C_p(\lambda, \beta) \quad (7)$$

C_p is basically mapping of complex behavior of wind turbine while operation. There are various ways to model C_p

characteristics of a specific wind turbine. The mathematical modelling of C_p as function of TSR and β is given [31, 33].

$$C_p(\lambda, \beta) = c_1 \left(\frac{c_2}{\lambda_i} - c_3 \beta - c_4 \right) \exp \left(-\frac{c_5}{\lambda_i} \right) + c_6 \lambda \quad (8)$$

Where

$$\lambda_i = \lambda + 0.08\beta - \frac{\beta^3 + 1}{0.035} \quad (9)$$

and c_1, c_2, c_3, c_4 and c_5 are aerodynamic constants for the curve of power coefficient.

Figure 2 shows the C_p characteristics of wind turbine at different values of blade pitch.

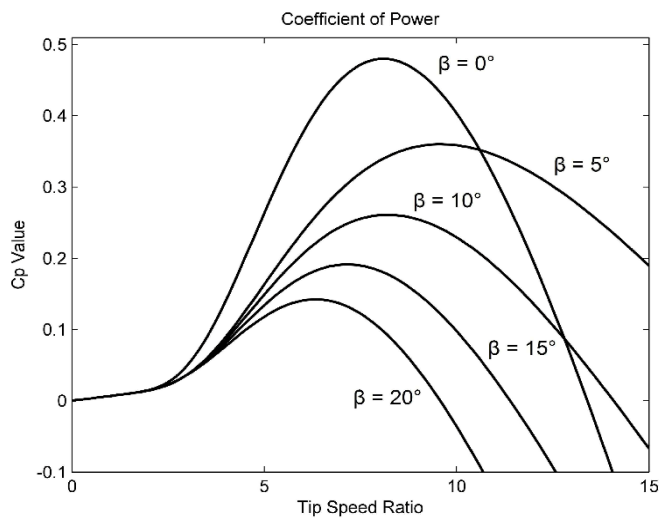


Fig. 2. C_p characteristics at different values of β

This type of complex behavior for C_p characteristics shown in Figure 3 may be modelled using 'Lookup Table' block of Simulink.

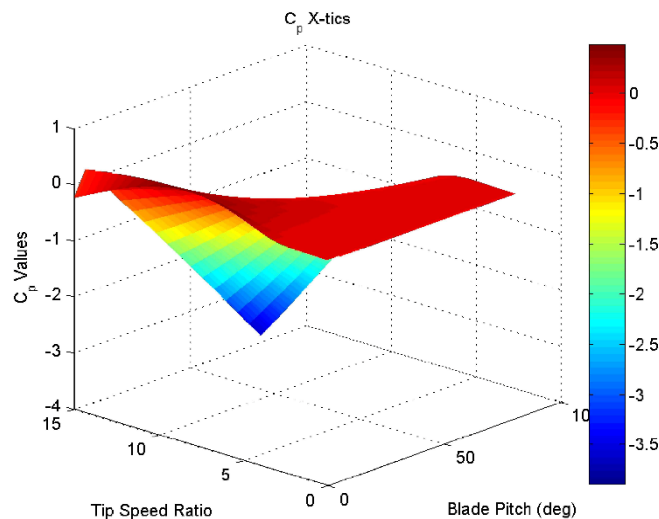


Fig. 3. C_p behavior modelled at variable β

The shaft speed characteristics is also a modelling of complex behavior of wind turbine against variable blade pitch and wind speed. This mapping becomes simpler when site is assumed with constant wind speed. Figure 4 shows the shaft speed characteristics of wind turbine.

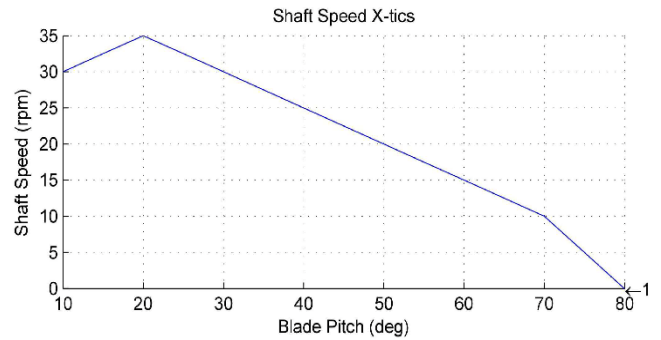


Fig. 4. Shaft speed behavior of wind turbine

Generally, the conventional wind turbine functions at low shaft speed [8]. The modern large wind turbine system itself includes the gear box and generator inside a nacelle for torque and speed conversion. The power on turbine side remains constant as that of generator side.

$$P_t = P_g \quad (10)$$

Mechanical power is articulated as torque time's shaft speed on the same end (turbine or generator side).

$$\tau_t \omega_t = \tau_g \omega_g \quad (11)$$

Thus the value of mechanical torque applied by wind turbine at generator shaft is given by: [31]

$$\tau_g = \frac{\tau_t \omega_t}{\omega_g} = \frac{P_t}{\omega_g} \quad (12)$$

2.2. Synchronous Generator

The WES consists of wind turbine coupled with 3-phase synchronous generator block of SimPowerSystems toolbox. The generator is set at ratings to feed maximum of 2 MW load at 50 Hz supply frequency and 11kV terminal voltage. The output terminal voltage of generator are maintained at constant level by using Excitation block. The generator has been modelled by using conventional d-q equations presented in [34, 35].

The synchronous generator represents the electromechanical energy conversion device. The mechanical model of synchronous generator is given by: [34, 35]

$$\Delta\omega(t) = \frac{1}{2H} \int_0^t (T_m - T_e) dt - K_d \Delta\omega(t) \quad (13)$$

$$\omega(t) = \Delta\omega(t) + \omega_0 \quad (14)$$

The rated parameters and specifications of WES (wind turbine and electrical generator) modelled for the current research, are given in Table 1. [9]

Table 1. Rated parameters of WES

Parameter	Value
Rated Power	2 MW
Rated Shaft Speed (n) of Wind Turbine	33 rpm or

	3.46 Rad/s
Rotor Radius of Wind Turbine	27 m
Air Density	1.225 Kg/m ³
Rated Wind Speed (V _w)	16 m/sec
Cut-in Wind Speed	8 m/sec
Power Coefficient (C _p)	0.35
Tip Speed Ratio (λ)	5~6
Blade Length (R)	27 m
Rated Blade Pitch (β)	24 deg
Maximum Blade Pitch	104 deg
Rated Rotor Speed of Generator	1500 rpm

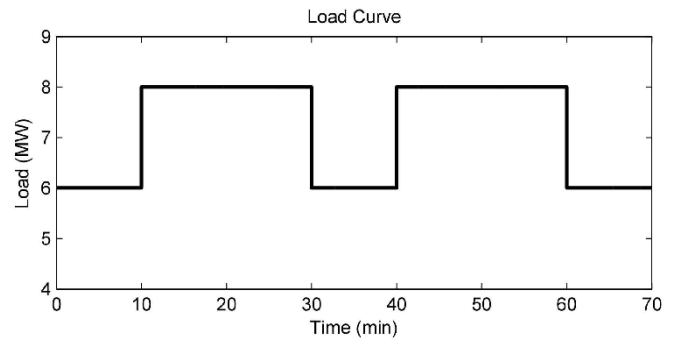


Fig. 6. Specified load curve

The block diagram of wind turbine modelling is shown in Figure 5.

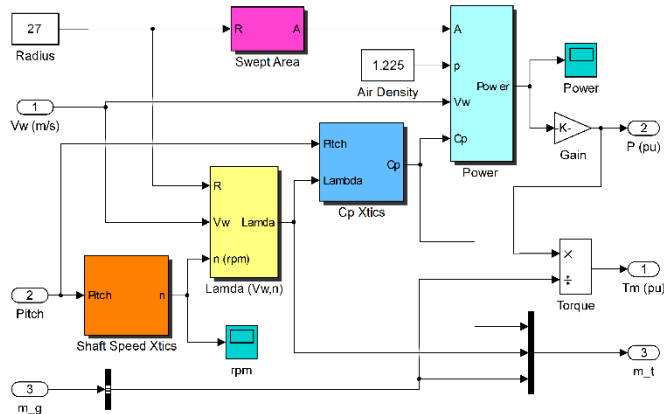


Fig. 5. Model of wind turbine

3. Modelling of National Grid Supply (NGS)

The national grid for the current case study has been proposed to start at 132kV grid station which is feeding 11kV substation through 25 km transmission line of 132kV. The 11kV substation steps down the voltage to 11kV through power transformer of 132kV/11kV. A 5 km long, 11kV distribution line (feeder) supplies the load at consumer end. The national grid supplies the 6 MW load at consumer end in peak load hours as well as in off-peak load hours.

4. Modelling of Variable Electrical Load (VEL)

The WES and NGS deliver the consumer end load which may also be referred as electrical load on both of the systems. The VEL is basically time varying load which is composed of two components: base load (6 MW) and peak load (2 MW). The base component of VEL remains connected to bus bar B4 all the time during peak as well as off-peak hours. The peak load component of VEL is switched through a 3-phase circuit breaker during peak load hour only. The circuit breaker is switched ON or OFF after receiving the signal from load management unit. The load curve considered for this case study is shown in Figure 6.

5. Load Management Unit (LMU)

The load allocation and operating conditions of WES, VEL, and Fuzzy Logic Controller are determined and sent by LMU. The LMU makes the Fuzzy Logic Controller to sense the load variations and directs the WES to take up the extended load demand during peak load hour. Before this, LMU specifies the load switching intervals for VEL to switch ON or OFF the peak load component. Thus LMU behaves like a central control system which coordinates with the whole system and makes the systems act consequently.

6. Fuzzy Logic Controller (FLC)

The key purpose of FLC is to load and unload the WES against VEL connected on bus bar B4 together with NGS. The FLC quashes the extreme and detrimental transients in the output power curve while loading of WES during peak load hour. Similar action is taken by FLC while unloading of WES during off-peak hour. The fuzzy logic control is an efficient control technique used for PFC application of WES. According to fuzzy logic, the blade pitch angle is expressed as function of peak occurrence/fall instants and rate of change of peak rise/fall against variations in load gradient which is given by: [36-38]

$$\beta(\Delta P_e; p_o, p_f, \gamma_{pr}, \gamma_{pf}) = \Delta P_e \times \left[\frac{1}{1 + \exp[p_o(t - \gamma_{pr})]} \times \frac{1}{1 + \exp[p_f(t - \gamma_{pf})]} \right] \quad (15)$$

The FLC activates/triggers itself among the system when there exists error signal which is load gradient. The LMU signals the operational parameters to FLC which keeps wait to activate itself by taking feedback of load gradient. Whenever peak occurs, FLC senses the load gradient higher than zero and loads the WES against VEL by changing the blade pitch slowly during peak hour. In the off-peak scenario, the FLC unloads the WES against VEL during off-peak hour to minimize the error signal to zero. The block diagram, shown in Figure 7, represents the logic of FLC during loading and unloading in peak and off-peak hours respectively.

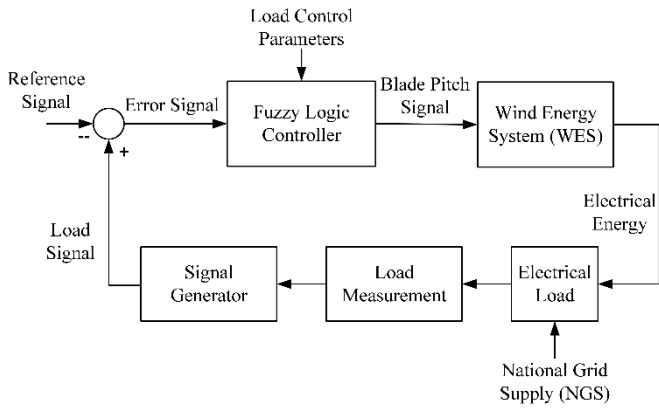


Fig. 7. Schematic diagram of FLC

7. Simulation

The simulation diagram of case study has been completed by modelling of WES, NGS, LMU, VEL and FLC. The comprehensive modelling follows the single diagram of whole system which is shown in Figure 8. From the diagram, FLC is connected between WES and bus bar B4. The WES is loaded and unloaded after sensing load gradient by FLC during peak and off-peak hours. According to case study, the base load of 6 MW is always fed by NGS while occurrence of extended load component during peak hour is shared by WES.

All the models of WES, LMU, NGS, FLC and VEL has been implemented in Simulink. The LMU is given with required information to communicate with other subsystems of simulation. This specific data includes the commands of peak occurrence and peak fall instants, and rates of change of peak occurrence and peak fall in peak and off-peak hours. The simulation block diagram is shown in Figure 9.

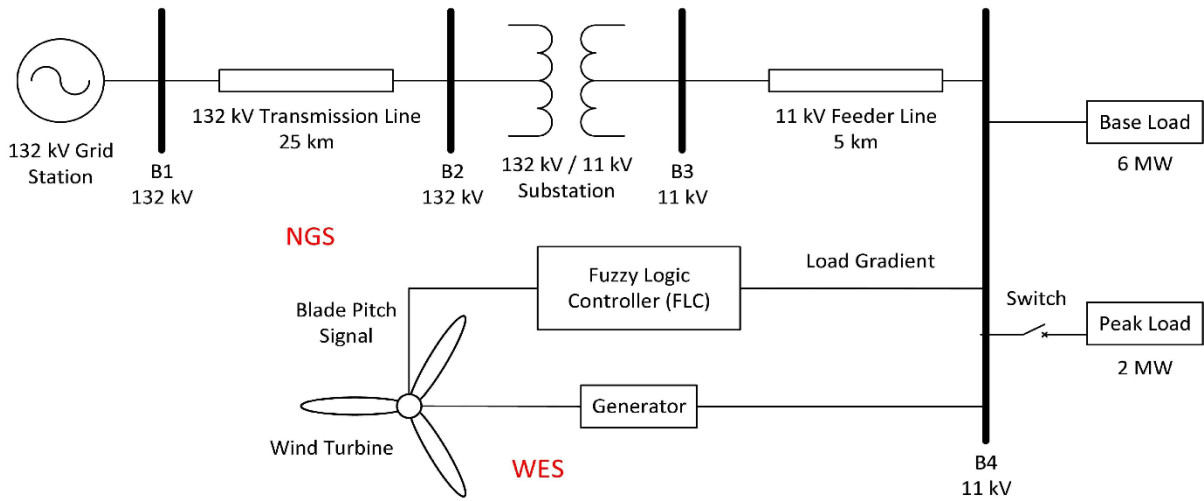


Fig. 8. Single line diagram of case study

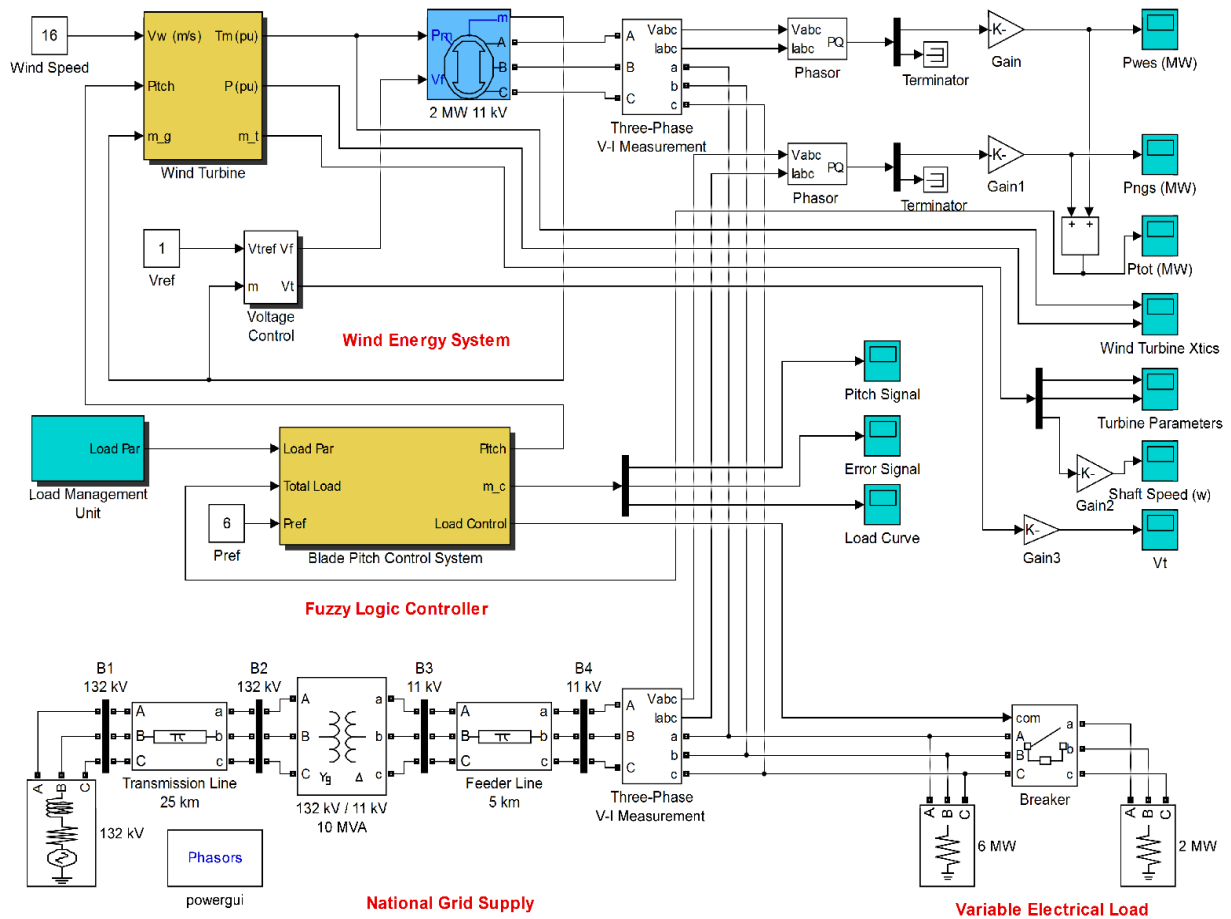


Fig. 9. Block diagram of case study

8. Simulation Results

8.1. Performance Analysis of WES and FLC for Discrete Time peak load Sharing

The simulation model has been run for 70 min (1 hour 10 minutes) time scale in Simulink environment. The system has been decreed for occurrence of two peaks of 20 min length each. The first peak occurs at 10 min instant and falls at 30 min instant whereas the second peak rises at 40 min instant and ends up to 60 min instant. The load shared by WES on bus bar B4 is 2 MW only in peak load hours. The Figure 10 shows that WES feeds the load only during peaks, 10 – 30 min and 40 – 60 min, otherwise it does not feed the load.

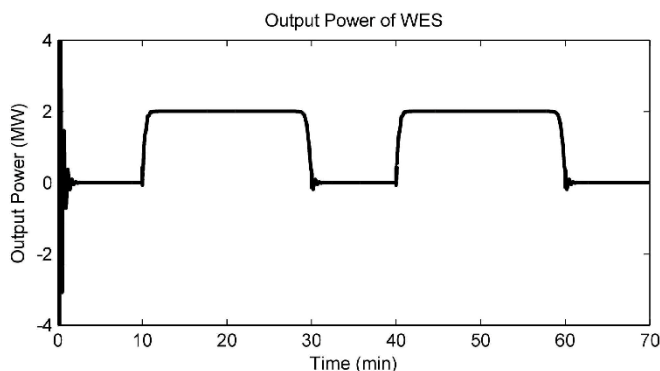


Fig. 10. Load shared by WES

The NGS feeds the base component of VEL constantly during peak as well as off-peak hours. However, small kinks can be seen in the output power curve of NGS because of loading and unloading of WES. Although the power supplied by NGS remains constant which is shown in Figure 11.

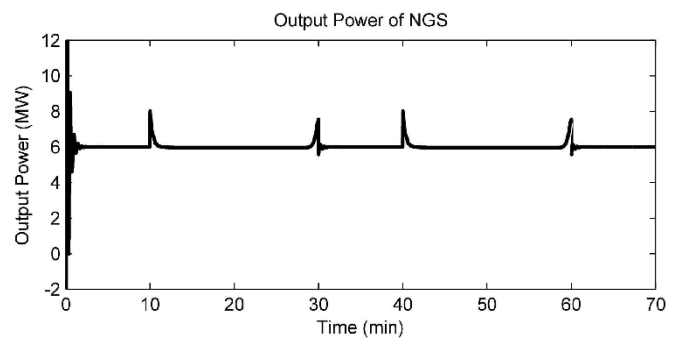


Fig. 11. Load supplied by NGS

The output power of both WES and NGS is shown in Figure 12 which represents complete load curve of system. The shown graph exhibits the peak of 8 MW and base of 6MW.

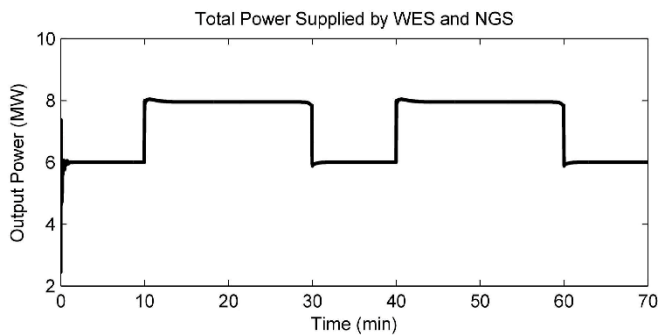


Fig. 12. Total load supplied by WES and NGS

During operation of WES, the PFC concept has to be implemented by which frequency of generator has to be maintained at constant level. The shaft speed regulation of wind turbine and electrical generator is the prerequisite of PFC. The shaft speed of generator has been demonstrated in Figure 13 which shows that generator turns at constant speed of 1500 rpm.

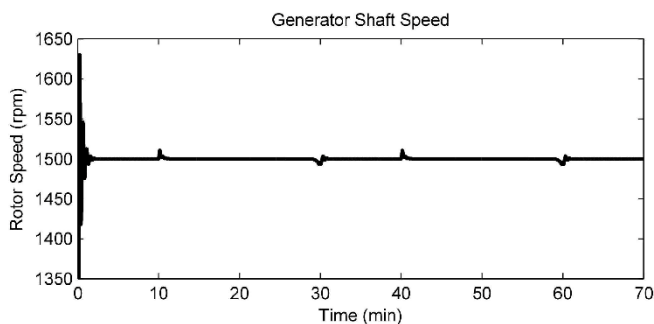


Fig. 13. Shaft speed of generator

The excitation subsystem has been employed for the generator to standardize the terminal voltage at perpetual level of 11kV. The following Figure 14 shows that generator terminal voltage remains at unceasing level.

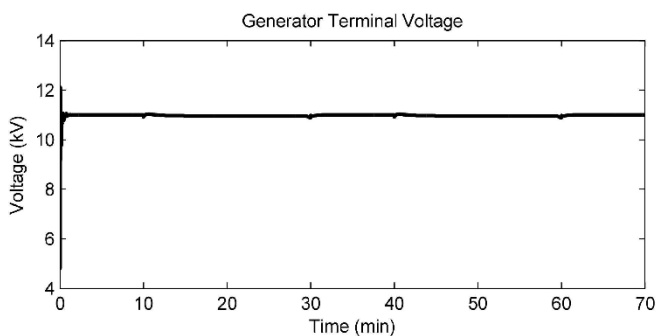


Fig. 14. Terminal voltage of generator

As WES has to take up the load in peak hour and take off the load in off-peak hour: the output mechanical torque and mechanical power have to be increased and decreased accordingly. The characteristics of wind turbine are shown in Figure 15 which expresses the behavioral change in mechanical torque and power in coordination with occurrence of peaks.

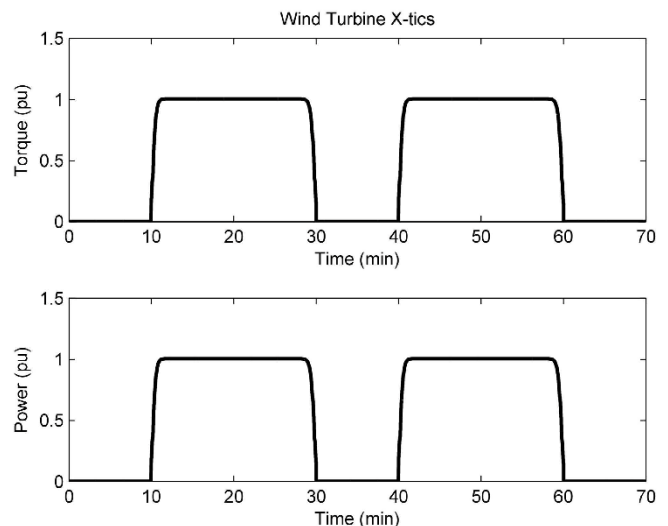


Fig. 15. Output torque and power of wind turbine in p.u.

The FLC sends the blade pitch control signal to WES to run accordingly. Actually FLC varies the value of blade pitch parameter slowly and smoothly so that wind turbine corresponds with the system change caused by VEL. The maximum and minimum ranges of blade pitch value are 104° and 24° where WES unloads and load itself respectively. At the instant of occurrence of peak, FLC changes the pitch signal from 104° to 24° and vice versa. Thus blade pitch signal sent by FLC to WES is shown in Figure 16.

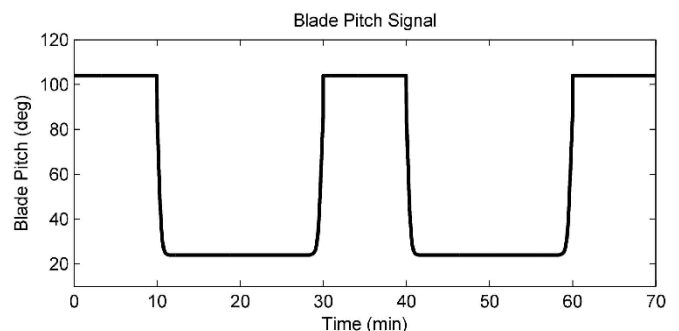


Fig. 16. Blade pitch signal generated by FLC

Generally, the control system drives itself into the system when there is change in error signal. In current research, the error signal is power mismatch: the value of which evolves with occurrence of peak load and diminishes in the absence of peak load. The error signal generated by FLC is shown in Figure 17.

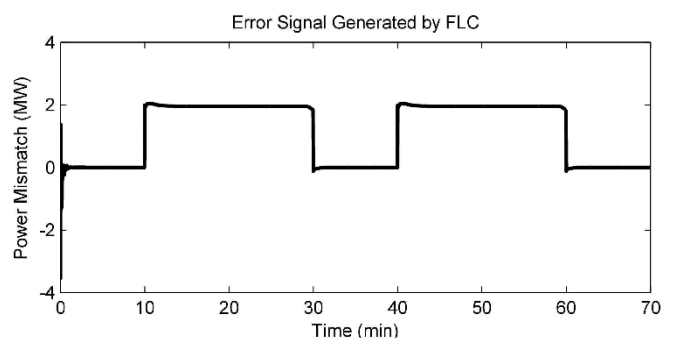


Fig. 17. Error signal of FLC

The various parameters of wind turbine at transition of VEL, indicates the system dynamics as FLC corresponds the WES. These parameters include C_p characteristics and TSR behavior. At the time of occurrence and falling of peak load, the dynamics of C_p is shown in Figure 18. The values of C_p and TSR vary during the operation of WES. The transients in TSR is shown in Figure 19 at loading and unloading instants of WES.

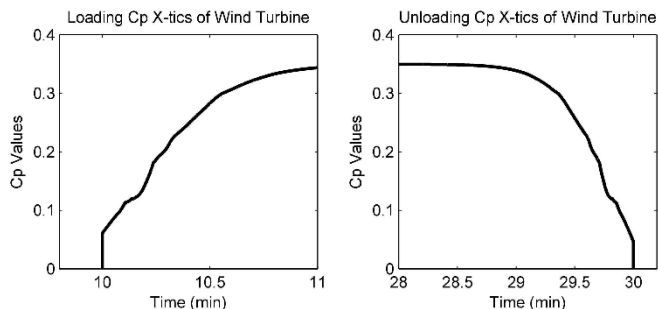


Fig. 18. C_p behavior of wind turbine while loading and unloading

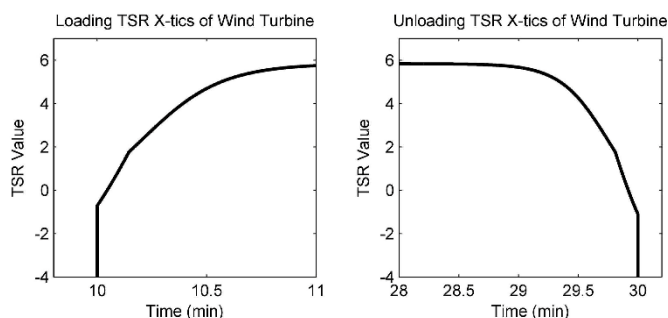


Fig. 19. TSR characteristics of wind turbine at loading and unloading instants

The Figure 20 shows the enlarged portion of output power of WES for transient analysis. The FLC has suppressed the transients in the curve to grander extent.

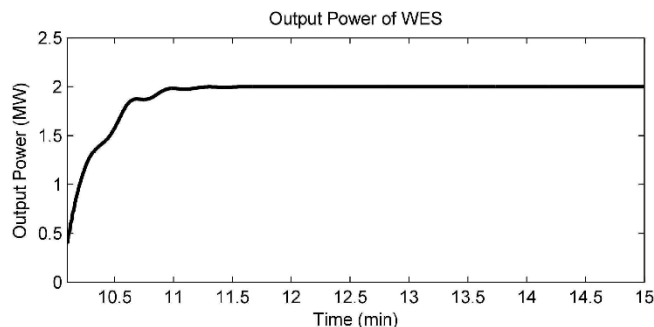


Fig. 20. Output power of WES at loading instant

The transient analysis resulted in computation of control parameter, percent overshoot, which comes out to be 1.0%. The value of percent overshoot depicts the performance of the FLC as compared to other controllers. The percent overshoot is 43% by using PID controller addressed in [25] whereas this value is 1.5% by using Blade Pitch Control (BPC) system presented in [9]. The comparison of results is listed in Table 2.

Table 2. Comparison of results

Parameter	Proposed FLC	BPC System [9]	PID Controller [25]
Percent Overshoot	1.0%	1.5%	43.0%

8.2. Performance of WES and FLC for Continuous Time Dynamic Load

In this case study the dynamic nature of domestic loads for one day (24 hours) is modelled keeping in view the conventional morning and evening peaks. In Pakistan, these peak hours usually occur from 0600-1000 hrs in the morning and 1800-2200 hrs in the evening. The aggregated behavior of domestic loads for different customers is represented as System Load curve and is shown in Figure 21(a).

The base load for NGS is 8MW and extended load of 2MW, which WES has to take up during peak hours, is investigated. The simulation model runs for 24 hour time scale axis to meet the required load. The Figure 21(b-d) explicitly show that WES and NGS successfully supply the expected variable load demand, according to the ratings defined for them, without causing any disturbance to the system. Moreover, it can also be observed that FLC equally work for continuous time load and the transients can hardly be seen.

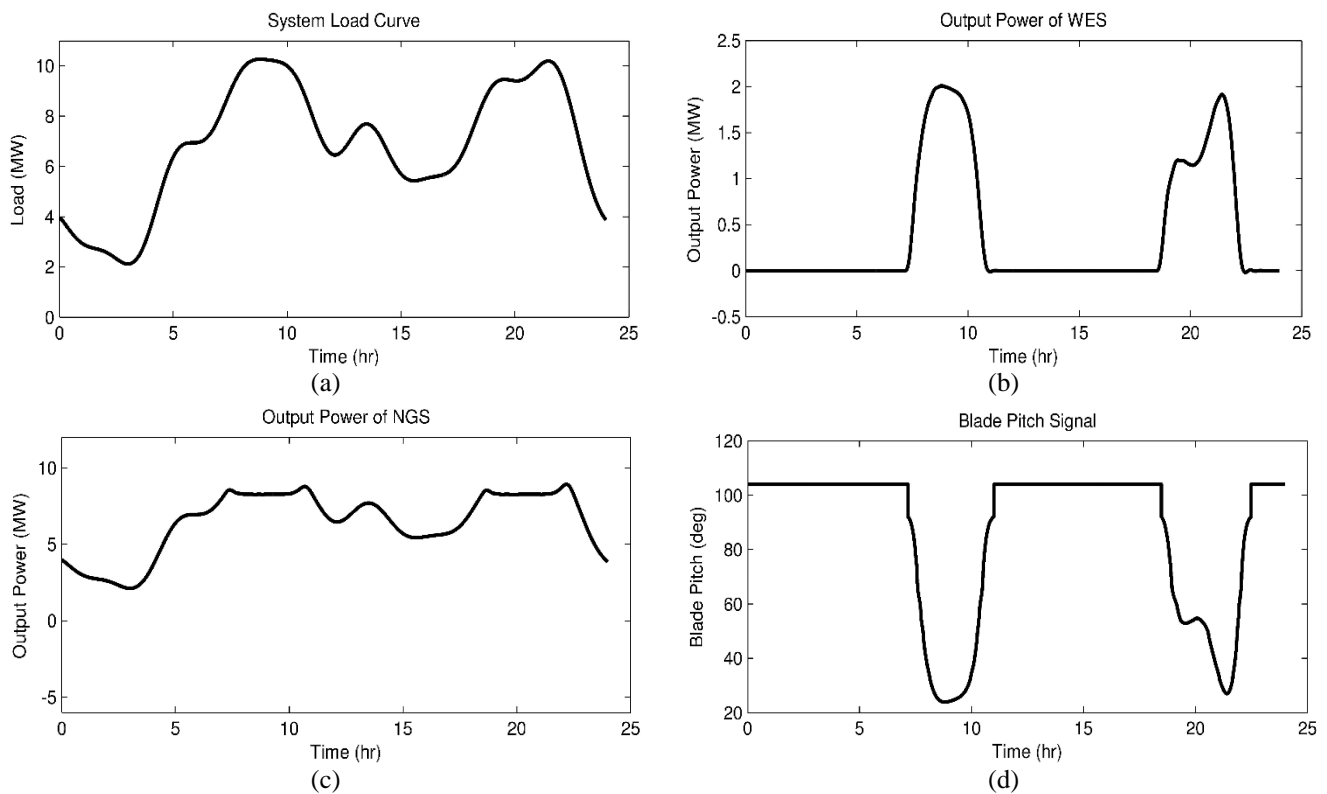


Fig. 21. Simulation Results for continuous time dynamic load: (a) System load curve, (b) Power supplied by WES, (c) Output power of NGS for base load, (d) FLC blade pitch signal

9. Conclusion

In this paper, a distributed generation system of wind energy is presented to meet the extended energy demand during peak hours. For this wind energy management System, fuzzy logic based control technique has been implemented and analyzed in terms of percent overshoot of the results. It is concluded that this independent controller can effectively work for any type of variable load and especially represents auspicious aspects while adopting with continuous variable load. The fine tuning of the control parameters guarantee with negligible amount of percent overshoot. Hence the proposed FLC proves to be promising and cost effective control technique as it decreases the consumption of fossil fuels and air pollution, load elimination and peak elimination. Moreover, without using electronic components such as converters/inverters, it exhibits extra energy to main network and participate in energy market and helps in economy of the country. However, the contribution of wind energy to supply is random which may increase the cost, emissions and lower efficiency due to more frequent switching of other plants when the wind drops and demand is still high.

Notations

P_m	Output mechanical power of wind turbine (W)
ρ_a	Air density (kg/m^3)
A	Swept area of wind turbine's propeller (m^2)
V_w	Wind speed (m/sec)
C_p	Power coefficient
λ	Tip speed ratio

β	Blade pitch (deg)
R	Blade length of wind turbine (m)
V_T	Blade tip speed (m/sec)
n	Shaft speed of wind turbine (rpm)
P_t	Power at wind turbine shaft (W)
P_g	Power at generator shaft (W)
τ_t	Torque at wind turbine shaft (Nm)
τ_g	Torque at generator shaft (Nm)
ω_t	Speed of wind turbine shaft (rad/sec)
ω_g	Speed of generator shaft (rad/sec)
$\Delta\omega$	Variation in angular speed of rotor (rad/sec)
H	Inertia constant
T_m	Mechanical torque (Nm)
T_e	Electromagnetic torque
K_d	Damper factor
ω_o	Rated angular speed of rotor (rad/sec)
ΔP_e	Load gradient (MW)
p_o	Peak occurrence instant
p_f	Peak fall instant
t	Simulation time
γ_{pr}	Rate of change of peak rise
γ_{pf}	Rate of change of peak fall

Acknowledgements

The authors would like to acknowledge the Advanced Power System Laboratory, Electrical Engineering Department, University of Engineering and Technology Taxila, Pakistan for providing lab resources to conduct the research.

References

- [1] B. K. NAICK, "Fuzzy Logic Controller based PV System Connected in Standalone and Grid Connected Mode of Operation with Variation of Load," *International Journal of Renewable Energy Research (IJRER)*, vol. 7, pp. 311-322, 2017.
- [2] N. S. Mubenga, "Grid connected solar photovoltaic in island states: Challenges, opportunities and waste management," in *Renewable Energy Research and Applications (ICRERA), 2015 International Conference on*, 2015, pp. 1332-1336.
- [3] M. M. Ashraf, T. N. Malik, and M. Iqbal, "Development of a Prototype Micro Wind Energy System with Adjustable Blade Pitch for Experimentation Purposes at Laboratory Level," *Nucleus*, vol. 51, pp. 75-86, 2014.
- [4] A. Jarral, M. Ali, M. H. Sahir, and R. A. Pasha, "Design Optimization and Analysis of Vertical Axis Wind Turbine Blade," *Nucleus*, vol. 50, pp. 7-12, 2013.
- [5] A. Amini and M. Kamoona, "Hidden wind farms potential for residential households having roof-mounted wind arrester," in *Renewable Energy Research and Application (ICRERA), 2014 International Conference on*, 2014, pp. 891-896.
- [6] M. Caruso, A. Di Tommaso, F. Genduso, R. Miceli, G. R. Galluzzo, C. Spataro, and F. Viola, "Experimental characterization of a wind generator prototype for sustainable small wind farms," in *Renewable Energy Research and Applications (ICRERA), 2016 IEEE International Conference on*, 2016, pp. 1202-1206.
- [7] Ö. Kiymaz and T. Yavuz, "Wind power electrical systems integration and technical and economic analysis of hybrid wind power plants," in *Renewable Energy Research and Applications (ICRERA), 2016 IEEE International Conference on*, 2016, pp. 158-163.
- [8] O. Anaya-Lara, N. Jenkins, J. Ekanayake, P. Cartwright, and M. Hughes, *Wind Energy Generation Modelling and Control*. West Sussex, United Kingdom: John Wiley & Sons, Ltd, 2009.
- [9] M. M. Ashraf, T. N. Malik, and M. Iqbal, "Peak load sharing based on blade pitch control of wind turbine in the presence of utility supply," *Journal of Renewable and Sustainable Energy*, vol. 6, p. 013110, 2014.
- [10] Z. H. Kamali, Z. Salameh, and A. Ashfaq, "Modeling of wind energy conversion system using PSCAD/EMTDC," *International Journal of Renewable Energy Research*, vol. 7, pp. 178-187, 2017.
- [11] M. Van Dessel, M. Gay, and G. Deconinck, "Simulation of grid connected PM generator for wind turbines," in *IEEE International Symposium on Industrial Electronics (ISIE)*, 2010, pp. 1479-1484.
- [12] W. Haining, C. Nayar, S. Jianhui, and D. Ming, "Control and Interfacing of a Grid-Connected Small-Scale Wind Turbine Generator," *IEEE Transactions on Energy Conversion*, vol. 26, pp. 428-434, 2011.
- [13] W. Haining, C. Nayar, S. Jianhui, and D. Ming, "Control and interfacing of a grid-connected small scale wind turbine generator," in *Australasian Universities Power Engineering Conference (AUPEC)*, 2009, pp. 1-5.
- [14] L. Wei and L. Weiguo, "Key technologies analysis of small scale non-grid-connected wind turbines: A review," in *World Non-Grid-Connected Wind Power and Energy Conference (WNWEC)*, 2010, pp. 1-6.
- [15] R. Bharanikumar and A. N. Kumar, "Novel method of wind energy conversion system by incorporating permanent magnet generator and single stage AC-AC power converter," *Journal of Scientific & Industrial Research*, vol. 70, pp. 379-384, 2011.
- [16] A. Nagliero, R. A. Mastromauro, M. Liserre, and A. Dell'Aquila, "Synchronization techniques for grid connected wind turbines," in *35th Annual Conference of IEEE on Industrial Electronics (IECON '09)*, 2009, pp. 4606-4613.
- [17] O. C. Ozerdem, "A System for Connecting the Wind Turbines to Power Grid," in *IEEE International Electric Machines & Drives Conference (IEMDC '07)*, 2007, pp. 442-446.
- [18] N. Joshi and N. Mohan, "A Novel Scheme to Connect Wind Turbines to the Power Grid," *IEEE Transactions on Energy Conversion*, vol. 24, pp. 504-510, 2009.
- [19] R. Ahshan, M. T. Iqbal, and G. K. I. Mann, "Performance of a Controller for Small Grid Connected Wind Turbines," in *IEEE Electrical Power Conference (EPC '07), Canada*, 2007, pp. 490-495.
- [20] A. E. Haniotis, K. S. Soutis, A. G. Kladas, and J. A. Tegopoulos, "Grid connected variable speed wind turbine modeling, dynamic performance and control," in *IEEE Power Systems Conference and Exposition*, 2004, pp. 759-764.
- [21] T. Porselvi and R. Muthu, "Design of Buck-Boost Converter for Wind Energy Conversion System," *European Journal of Scientific Research*, vol. 83, pp. 397-407, 2012.
- [22] G. Munireddy, "Multi Level Inverter Based STATCOM for Grid Connected Wind Energy Conversion System," *International Journal of Renewable Energy Research (IJRER)*, vol. 7, pp. 80-87, 2017.

- [23] M. S. Hamad, K. Ahmed, and A. S. Abdel-Khalik, "Grid connected high power medium voltage wind energy conversion system with reduced line harmonics," in *Renewable Energy Research and Applications (ICRERA), 2015 International Conference on*, 2015, pp. 1279-1284.
- [24] D. K. VARMA and Y. Obulesh, "An Improved Synchronous Reference Frame Controller based Dynamic Voltage Restorer for Grid Connected Wind Energy System," *International Journal of Renewable Energy Research (IJRER)*, vol. 6, pp. 880-888, 2016.
- [25] S. Jie, Z. Yaliang, F. Wenxiu, and Z. Xin, "Research on advanced control strategies for wind turbine variable-pitch system," in *25th Chinese Control and Decision Conference (CCDC)*, 2013, pp. 390-395.
- [26] L. Y. Wang, J. Meng, and T. Zhang, "An intelligent variable pitch angle control approach in grid connected wind turbine," in *International Conference on Electric Information and Control Engineering (ICEICE)*, 2011, pp. 2958-2961.
- [27] S. Joshi, A. Patel, P. Patel, and V. Patel, "Wind Energy - A Brief Survey With Wind Turbine Simulations," *International Journal of Computer Communication and Information System (IJCCIS)*, vol. 2, pp. 228-232, July-Dec 2010 2010.
- [28] W. Nation. (2010). *Tip Speed Ratio: How to Calculate and Apply TSR to Blade Selection*. Available: <http://www.windnation.com/articles/wind/tip-speed-ratio-how-calculate-and-apply-tsr-blade-selection>
- [29] H. Stiesdal. (1999) *The Wind Turbine Components and Operation. Bonus Info*. Available: <http://users.wpi.edu/~cfurlong/me3320/DProject/Bonus Energy-1998.pdf>
- [30] T. Ackermann, *Wind power in power systems* vol. 140: Wiley Online Library, 2005.
- [31] S. Evren, M. Ünel, M. F. Akşit, and I. Tuzla, "MODELING AND CONTROL OF A VARIABLE SPEED VARIABLE PITCH ANGLE PROTOTYPE WIND TURBINE," *Mathematical and Computational Applications*, vol. 18, pp. 408-420, 2013.
- [32] S. Lain, B. Quintero, and Y. López, "Aeromechanical evaluation of large HAWT's blades," *Journal of Scientific & Industrial Research*, vol. 69, pp. 142-145, 2010.
- [33] B. Gilev, J. Slavchev, D. Penev, and A. Yonchev, "Model and Predictive Control for a Wind Turbine," in *Proceedings of AIP Conference*, 2011, p. 15.
- [34] P. C. Krause, *Analysis of Electric Machinery*: McGraw Hill, 1986.
- [35] I. Kamwa, M. Pilote, P. Viarouge, B. Mpanda-Mabwe, M. Crappe, and R. Mahfoudi, "Experience with computer-aided graphical analysis of sudden-short-circuit oscillograms of large synchronous machines," *IEEE Transactions on Energy Conversion*, vol. 10, pp. 407-414, 1995.
- [36] J. M. Mendel, "Fuzzy logic systems for engineering: a tutorial," *Proceedings of the IEEE*, vol. 83, pp. 345-377, 1995.
- [37] S. Sivanandam, S. Sumathi, and S. Deepa, *Introduction to fuzzy logic using MATLAB* vol. 1: Springer, 2007.
- [38] I. MathWorks and W.-c. Wang, *Fuzzy Logic Toolbox: for Use with MATLAB: User's Guide*: MathWorks, Incorporated, 1998.